



Determination of Exposure during Handling of ^{125}I Seed Using Thermoluminescent Dosimeter and Monte Carlo Method Based on Computational Phantom

Hosein Poorbaygi¹, Seyed Mostafa Salimi², Falamarz Torkzadeh¹, Saeid Hamidi², Shahab Sheibani¹

¹Applied Radiation Research School, Nuclear Science and Technology Research Institute, Tehran, Iran; ²Departments of Physics, University of Arak-Sardasht Campus, Arak, Iran

ABSTRACT

Background: The thermoluminescent dosimeter (TLD) and Monte Carlo (MC) dosimetry are carried out to determine the occupational dose for personnel in the handling of ^{125}I seed sources.

Materials and Methods: TLDs were placed in different layers of the Alderson-Rando phantom in the thyroid, lung and also eyes and skin surface. An ^{125}I seed source was prepared and its activity was measured using a dose calibrator and was placed at two distances of 20 and 50 cm from the Alderson-Rando phantom. In addition, the Monte Carlo N-Particle Extended (MCNPX 2.6.0) code and a computational phantom with a lattice-based geometry were used for organ dose calculations.

Results and Discussion: The comparison of TLD and MC results in the thyroid and lung is consistent. Although the relative difference of MC dosimetry to TLD for the eyes was between 4% and 13% and for the skin between 19% and 23%, because of the existence of a higher uncertainty regarding TLD positioning in the eye and skin, these inaccuracies can also be acceptable. The isodose distribution was calculated in the cross-section of the head phantom when the ^{125}I seed was at two distances of 20 and 50 cm and it showed that the greatest dose reduction was observed for the eyes, skin, thyroid, and lungs, respectively. The results of MC dosimetry indicated that for near the head positions (distance of 20 cm) the absorbed dose rates for the eye lens, eye and skin were 78.1 ± 2.3 , 59.0 ± 1.8 , and 10.7 ± 0.7 $\mu\text{Gy/mCi/hr}$, respectively. Furthermore, we found that a 30 cm displacement for the ^{125}I seed reduced the eye and skin doses by at least 3- and 2-fold, respectively.

Conclusion: Using a computational phantom to monitor the dose to the sensitive organs (eye and skin) for personnel involved in the handling of ^{125}I seed sources can be an accurate and inexpensive method.

Keywords: Occupational Dose, ^{125}I Seed, Exposure, Computational Phantom, Thermoluminescent Dosimeter, Monte Carlo Simulation

Original Research

Received July 21, 2023
Revision October 6, 2023
Accepted October 23, 2023

Corresponding author:

Hosein Poorbaygi

Applied Radiation Research School,
Nuclear Science and Technology
Research Institute, North Kargar Ave,
Tehran 14395-836, Iran
E-mail: hpoorbaygi@gmail.com

<https://orcid.org/0000-0001-9644-8587>

This is an open-access article distributed under the terms of the Creative Commons Attribution License (<http://creativecommons.org/licenses/by-nc/4.0/>), which permits unrestricted use, distribution, and reproduction in any medium, provided the original work is properly cited.

Copyright © 2023 The Korean Association for Radiation Protection

Introduction

In recent years, brachytherapy has been considered for brain tumors and is used in many large neurosurgery centers [1, 2]. In this treatment, ^{125}I seeds with activity between 10 and 20 mCi are used. Brachytherapy is an accepted treatment for the treatment of choroidal melanomas to preserve the globe, vision, and quality of life. For the

^{125}I plaque, 20 to 24 seed sources are used, and each seed has an activity of 4 to 6 mCi [3]. Brachytherapy of the prostate with ^{125}I seed is the standard radiotherapeutic approach and is increasing in importance [4–7].

Cattani et al. [4] state that the radiation exposure to the patient's relatives is below the legal threshold. Several studies have focused on studying occupational doses related to the implant of ^{125}I seed during prostate implants [5–8]. The dose equivalent $H_p(10)$ and $H_p(0.07)$, of less than 30 and 420 μSv per application were measured during prostate brachytherapy with ^{125}I seed [5]. Schiefer et al. [8] studied the radiation exposure of the physician during prostate seed implantation. However, there are few studies to determine the trend in occupational doses received from the ^{125}I ocular plaque during brachytherapy procedures [9, 10]. Al-Haj et al. [9] determined the occupational doses of ^{125}I ocular plaque received during the procedure and compared them with other published data.

Souza et al. [11] evaluated the risks to which workers are exposed during the production and handling of the ^{125}I seed sources. Despite the extensive studies mentioned above, little research has been done on the occupational doses received by the eyes and head skin during the ^{125}I seed implantation procedure. For occupational exposure, the revised equivalent dose limits for the lens of the eye are 20 mSv in a year. Thus, continuous review of eye lens doses of the workers during medical procedures is recommended [12, 13]. The 15 mSv limit has been considered adequate for protection against deterministic effects, although there is some consideration being given at present to reducing this limit in light of more information on visual impairment [14]. Publications from the International Atomic Energy Agency (IAEA) [12], International Organization of Standardization [15], and International Radiation Protection Association [16] recommend routine monitoring above 5 or 6 mSv per year. However, consistent with the as low as reasonably achievable (ALARA) principle, doses should always be minimized as much as possible. Dose assessment using physical phantoms has been carried out for quite some time in brachytherapy.

In recent years, ^{125}I brachytherapy sources have been used for brain tumors and the treatment of choroidal melanomas in our country using home-made ^{125}I seed [3]. However, our experience during the quality control of ^{125}I seed and the seed implantation during the treatment procedure has shown that there is occupational exposure to the head and neck area, and the radiation protection design is required. Therefore, a

computational phantom (VIP-Man model) [17] has been used for dose determination purposes in the head and neck organs, particularly for the eye lens. In the field of safety, handling ^{125}I seed and implantation of seed can be a new approach.

In this study, the primary aim is to evaluate the absorbed dose values of personnel during quality control of low dose rate (LDR) seed sources as well as the dose delivered to the nurse and the physician during ^{125}I seed implantation, such as treatment of a brain tumor or ocular tumor. Furthermore, we demonstrate that the computational method can be used as a reasonable and cost-effective alternative, compared to the experimental approach and the use of the thermoluminescent dosimeter (TLD) and Alderson-Rando phantom for validation of the Monte Carlo (MC) computational model.

Materials and Methods

1. Radioactive Source, Phantom, and Dosimeter Specifications

The ^{125}I seed source is a proprietary product, and its dosimetric parameters were measured by two groups in accordance with the American Association of Physicists in Medicine Task Group no. 43 (AAPM-TG-43) formalism [18, 19]. It was encapsulated by titanium (4.7 mm in length, 0.8 mm in outer diameter, and 4.54 g/cm³ in density) by 15-W Nd:YAG laser welding. The activity of the brachytherapy seed was measured using a dose calibrator (CRC-15BT; Mirion Technologies), which was 15.4 mCi.

An Alderson-Rando phantom is used for the experiment setup. This phantom is proportionally equivalent to an average human with a height of 1.75 m and a weight of 73.5 kg, which is equivalent to tissue. The phantom is cut to a thickness of 25 mm, and each phantom contains a matrix of 5 mm-diameter holes.

A TLD or Perspex chip (Jumei Acrylic Manufacturing Co., Ltd.) equivalent to tissue can be placed in each cavity. We used LiF:Mg, and Ti (TLD-700) chips to monitor the organ dose. The TLD-700 (⁶Li is 0.01% and ⁷Li is 99.99%) is used to measure the dose of gamma rays with dimensions of 3 mm × 3 mm × 0.9 mm [20]. This study employed the method of annealing and reading TLD chips described by Meigooni et al. [21]. The absorbed dose for each TLD is determined by the following equation:

$$D(\text{mGy}) = R(n\text{C}) \times ECC \times EF^{-1} \times CF^{-1} \left(\frac{\text{mGy}}{n\text{C}} \right) \times \frac{RL_0}{RL} \quad (1)$$

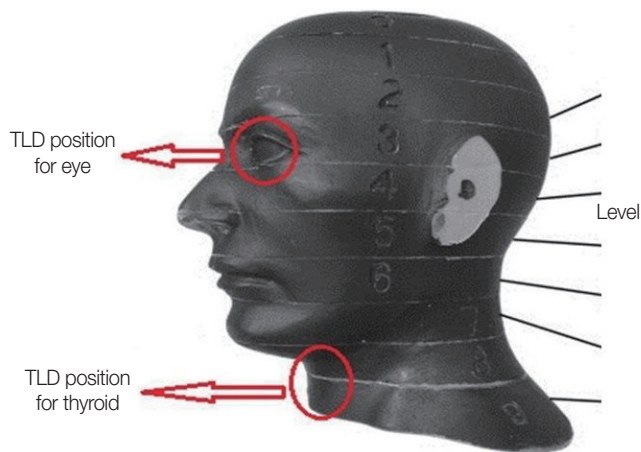


Fig. 1. Head of the Alderson-Rando phantom and the location of the thermoluminescent dosimeters (TLDs).

where D is the amount of absorbed dose, R is the amount of the reader output, ECC is the correction factor of the TLD chip, CF is the calibration factor of each TLD, EF is the energy correction factor for the source, RL_0 is the average value of Reference Light measured between TLD readings, and RL is the average value of reference light measured between TLD readings of which RL is 94.91. Finally, the background dose is subtracted from the dose that was obtained.

For calculating of dose, the VIP-Man head and torso phantom was used, which was created from transverse color photographic images [22]. Radiosensitive organs, such as the red bone marrow, have been segmented and labeled in the VIP-Man model for dose calculations. This phantom covers the portion of the body from the middle of the lungs to the top of the head. The voxel size is $4\text{ mm} \times 4\text{ mm} \times 4\text{ mm}$. We use a lattice-based geometry. The input deck is quite descriptive, and we can run it on a Windows system.

2. Experiment Design

To determine the occupational dose in the handling of ^{125}I seed this scenario was considered. LDR seeds for brachytherapy implants have been handled at distances between 5 and 35 cm, which correspond to 20 to 50 cm from the center axis of the phantom. Therefore, the ^{125}I seed was placed at 20 and 50 cm distances from the central axis of the Alderson-Rando phantom in the experimental work. The organ doses were measured by placing TLDs in various parts of the phantom. The sample preparation of TLDs was as follows. In each section, 27 TLDs were utilized. Four TLDs were placed in layer no. 15 of the Rando phantom in front of the chest muscle tissue, three TLDs in layer no. 14 in the lung area, two



Fig. 2. A layer of the torso part of the Alderson-Rando phantom and the location of the thermoluminescent dosimeters (TLDs).

TLDs in layer no. 12 on the inner surface of the skin. One TLD in layers no. 10 and three TLDs were placed in layer no. 9 in the thyroid area, three TLDs in the right eye area, three TLDs in the left eye area, and finally, five TLDs were placed on the layer of the outer surface of the skin. In order to put TLDs on the eyes and outer surface of the skin, they were first placed in a thin plastic bag and then attached to the phantom. Furthermore, we employed three TLDs as a background control in each step of the experiment. The axis of the seed source was considered at a distance of 20 cm from the central axis of the Rando phantom. This distance was equal to 4.5 cm from the nose tip of the phantom. The steps mentioned in the second section were exactly repeated and only a 50 cm distance was taken into account. Fig. 1 shows the picture of the Alderson-Rando phantom and the location of the TLD on the head and neck, and Fig. 2 shows the location of the TLDs into the torso portion layer. TLDs were placed in different layers of the Alderson-Rando phantom on the thyroid, lungs, eyes, and inner surface of the skin. The irradiation time was set at 20 hours and the TLD dose in each case was obtained using the mentioned method.

3. Monte Carlo Simulation

The MC simulations are carried out using the Monte Carlo N-Particle Extended (MCNPX 2.6.0) code, and Evaluated Nuclear Data File (ENDF)/B-VI cross-section libraries were used to simulate the particle interaction [23]. The several application fields of this code include medical physics, radiation protection, and dosimetry. The simulations with default parameters for the transmission of photons and electrons are done. To calculate organ doses, the VIP-Man phantom consisting of predefined organs is used. In the first step to validating MCNPX 2.6.0 code, modeling of the voxel phantom and defining the ^{125}I seed were done based on the geometry between the seed source and the TLD loaded in the

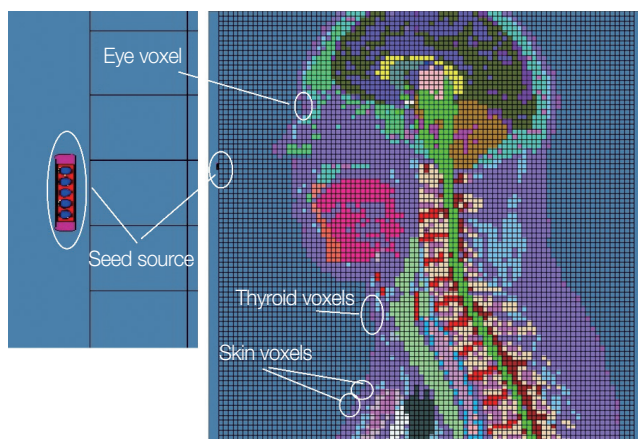


Fig. 3. Image of VIP-Man phantom with voxel tallies as thermoluminescent dosimeter and also ^{125}I seed source that was placed outside the phantom that was run by the Monte Carlo N-Particle Extended (MCNPX 2.6.0) code.

computational phantom was used in this simulation. For the two mentioned distances, i.e., 20 and 50 cm from the central axis of the computational phantom, the MCNPX 2.6.0 run was conducted. An image of the computation modeling in X-section (sagittal view) executed with the MCNPX 2.6.0 code is shown in Fig. 3. On the right side of this image, an ^{125}I seed was defined as containing and five resin spheres (5 mm in diameter) with a radioactive spherical layer and a cylindrical of titanium capsule (4.7 mm in length, 0.8 mm in outer diameter, and 4.54 g/cm^3 in density). The distance between the central axis of the seed and the central axis of the computational phantom was defined as 20 cm. The output from the MC calculation, was computed using the *F8 energy deposition tally in units of MeV/photon from the mesh tally and 8×10^7 number of histories. Finally, dose rate was calculated in units of cGy/mCi/hr. To perform more comprehensive dosimetry for different positions of the source from the central axis of the phantom, such as 20, 30, 40, and 50 cm, the MCNPX 2.6.0 code was run in the next step.

Results and Discussion

Table 1 displays the comparison of the MCNPX 2.6.0 dose results with the results of the TLD experiments for validating the MC simulation. The quantity of external irradiation caused by handling ^{125}I seed is shown by the dose values for the organs, which are shown in mGy. The statistical uncertainties (type A) due to repetitive TLD measurements are found to be 7%, 4%, 4%, and 16% for the eye, thyroid, lung and skin respectively. The uncertainties (type B) due to dose calibration

Table 1. Comparison of the Dose Values for Organs (mGy) for the Exposure of ^{125}I Seed (15.4 mCi) at 20 Hours at Two Distances (cm) by the TLD and MC Methods

| Organ | Distance (cm) | Dose (mGy) | | Relative difference (%) |
|---------|---------------|-------------------|------------------|-------------------------|
| | | TLD ^{a)} | MC ^{a)} | |
| Eyes | 20 | 20.37 (10) | 17.69 (3) | 13.1 |
| | 50 | 1.33 (8) | 1.38 (3) | 3.7 |
| Thyroid | 20 | 2.10 (8) | 2.02 (7) | 3.8 |
| | 50 | 0.83 (8) | 0.82 (7) | 2.4 |
| Lung | 20 | 0.71 (8) | 0.64 (9) | 9.9 |
| | 50 | 0.38 (8) | 0.36 (9) | 7.9 |
| Skin | 20 | 4.03 (18) | 3.20 (6) | 23.1 |
| | 50 | 0.91 (18) | 0.72 (6) | 18.7 |

The values within the brackets indicate the relative standard deviation (1σ) for dose value for organs and the value has a unit of percent. TLD, thermoluminescent dosimeter; MC, Monte Carlo.

and TLD positioning are found at 5% and 5% respectively. The total uncertainties for this dosimeter are calculated as 10%, 8%, 8%, and 18% for the eye, thyroid, lung and skin, respectively. Table 1 presents the uncertainties for the absorbed dose.

As can be seen, the experimental results and the values derived from MCNPX 2.6.0 in the thyroid and lung organs are consistent. However, the relative difference of MC dosimetry to TLD for the eyes is between 4% and 13% and for the skin between 19% and 23%. Fig. 4 shows the comparison of the absorbed dose for eye and skin using the TLD and MC methods and their uncertainties. Due to the higher uncertainty for TLD in eye and skin, as depicted in Fig. 4, these relative inaccuracies can be tolerated. The main reason for this relative difference could be due to the difference in the position of the TLD inside the Alderson-Rando phantom relative to the computational head phantom.

The diagram of the absorbed dose rate in grayscale levels and isodose obtained from the MCNPX 2.6.0 when the ^{125}I seed was placed at two distances of 20 and 50 cm from the central axis of the phantom is shown in Fig. 5. This diagram shows a Z cross-section (transverse plane) of the head phantom, which can be seen on the right side of the eye and nose cross sections. The value of each voxel is in cGy/hr per source particle. We use Tec-plot software (Tecplot Inc.) to draw isodoses. The red pixels show the areas with the highest dose (hot spots), and the blue pixels show the areas with the lowest dose. The greatest dose reduction is observed for the eyes, skin, thyroid and lungs, respectively. The results show that a 30 cm displacement for the ^{125}I seed reduces the eye dose and skin dose by at least about 12 and 4 times, re-

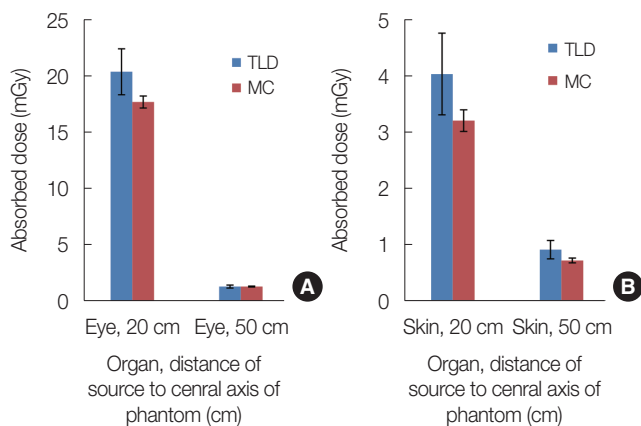


Fig. 4. Comparison of thermoluminescent dosimeter (TLD) and Monte Carlo (MC) absorbed doses and their uncertainties for (A) eye and (B) skin.

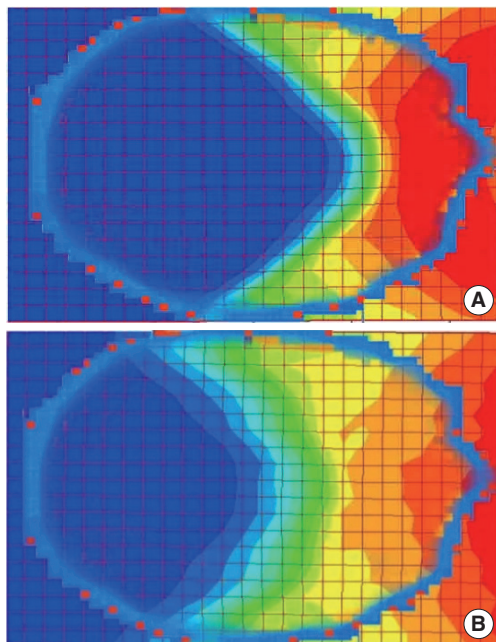


Fig. 5. Iso-doses distribution at Z cross-section (transvers plane) of the head phantom by the Monte Carlo N-Particle Extended (MCNPX 2.6.0) code for the occupational exposure from handling of ¹²⁵I seed. (A) The seed source is located in the distance of 20 cm from the central axis of the phantom. (B) The seed source is located in the distance of 50 cm from central axis of the phantom.

spectively.

For occupational dosimetry purposes, the ¹²⁵I seed was placed at a distance of 20, 30, 40, and 50 cm from the VIP-Man phantom. The calculated dose rates in terms of $\mu\text{Gy}/\text{mCi}/\text{hr}$ are given in Table 2. According to the results, we observed that the eye lenses receive the highest dose, followed by the skin layer, the thyroid, and finally the lungs. If there are no lead glasses on the eyes, the maximum exposure time of ¹²⁵I

Table 2. Absorbed Dose Rates ($\mu\text{Gy}/\text{mCi}/\text{hr}$) for ¹²⁵I Seed with the Activity of 1 mCi at Distances of 20 to 50 cm from the Central Axis of the Computational Phantom

| Organs | Distance (cm) | Dose ($\mu\text{Gy}/\text{mCi}/\text{hr}$) |
|--------------|---------------|--|
| Eyes | 20 | 59.0 (3) |
| | 30 | 19.5 (3) |
| | 40 | 89.7 (3) |
| | 50 | 4.9 (3) |
| | | |
| Eye lenses | 20 | 78.1 (3) |
| | 30 | 28.3 (3) |
| | 40 | 10.4 (3) |
| | 50 | 6.8 (3) |
| | | |
| Thyroid | 20 | 7.4 (9) |
| | 30 | 5.8 (9) |
| | 40 | 3.9 (9) |
| | 50 | 2.7 (9) |
| | | |
| Gray matter | 20 | 1.9 (3) |
| | 30 | 0.9 (3) |
| | 40 | 0.5 (3) |
| | 50 | 0.3 (3) |
| | | |
| White matter | 20 | 1.8 (3) |
| | 30 | 0.8 (3) |
| | 40 | 0.5 (3) |
| | 50 | 0.3 (3) |
| | | |
| Lung | 20 | 2.2 (9) |
| | 30 | 1.9 (9) |
| | 40 | 1.6 (9) |
| | 50 | 1.2 (9) |
| | | |
| Skin | 20 | 10.7 (6) |
| | 30 | 8.3 (6) |
| | 40 | 4.2 (6) |
| | 50 | 2.5 (6) |
| | | |

The value within the brackets indicate the relative standard deviation (1σ) for dose value for organs and the value has a unit of percent.

seed (activity of 15.4 mCi) can be estimated. Therefore, the maximum working time according to the weekly occupational limit, 1 mSv/week, will be about 1.2 and 13.4 hours for 20 and 50 cm distance, respectively.

Anglesio et al. [5] recorded the doses equivalent $H_p(10)$ and the equivalent dose $H_p(0.07)$ of less than 30 and 420 μSv using film and finger ring dosimeters during brachytherapy with the ¹²⁵I seed. Kaulich et al. [6] reported $H_p(0.07)$ values up to 1 mSv on the hands. In Table 1, we also reported a skin dose of about 298 μSv (for a time of 2 hours and a distance of 20 cm), which is in agreement with those reported by other authors for the finger dose. The use of lead gloves reduces the dose to the hands, and a reduction of about 50% in the received doses was observed.

The equivalent dose at a depth of 0.07 mm, $H_p(0.07)$, using TLD-100 (LiF:Mg, Ti) dosimeters for the physician's eye during interventional radiology was measured by Bahruddin et

al. [13]. They report a mean $H_p(0.07)$ dose of 0.33 mSv and 0.20 mSv for the left and right eye lenses, respectively. The eye lens radiation exposure was recorded in terms of the equivalent dose, $H_p(0.07)$, and the dose under the lead apron was recorded as $H_p(10)$. The effective dose was calculated based on the following equation:

$$E = 0.84 H_p(10) + 0.051 H_p(0.07) \quad (2)$$

Equation (2), known as the Von Boetticher algorithm, was derived based on International Commission on Radiological Protection 103 [13].

The IAEA recommended that for the mean photon energy below about 40 keV, $H_p(0.07)$ may be used but not $H_p(10)$. For non-homogeneous radiation fields, monitoring near the eyes is necessary. When protective equipment such as lead glasses is in use, monitoring near the eyes and below the protective equipment or an equivalent layer of material is necessary. Otherwise, appropriate correction factors to take the shielding into account should be applied. If a lead apron is used for the trunk, monitoring below the shielding underestimates the dose to the lens of the eye as the eye is not covered by the trunk shielding. However, separate monitoring near the eyes is necessary [14].

Quantifying the protection provided by lead glasses is difficult, and most dosimeters are not designed to be used under lead glasses [24]. In this study, we introduced a method to determine the absorbed dose for eyes (without lead glasses) using a computational phantom. It can be used to monitor the dose to the eye for personnel involved in the handling of ^{125}I seed. This data can be useful for designing the thickness of lead glasses suitable for working with ^{125}I seed.

Conclusion

The absorbed dose values for eyes, eye lens, thyroid, skin, and lung were evaluated using a computational phantom during the handling of ^{125}I seed. The TLD and the Alderson-Rando phantom were used to validate the MCNPX 2.6.0 code. The two-dimensional diagram of the absorbed dose rate in grayscale levels shows that the eye lenses and eyes receive the highest dose. Therefore, there is a need to move the source or reduce time, which was quantitatively evaluated in this study. The results indicated that for near the head (distance of 20 cm) the absorbed dose rate for the eye lens, eye and skin were 78.1 ± 2.3 , 59.0 ± 1.8 , and 10.7 ± 0.7 $\mu\text{Gy}/\text{mCi}/\text{hr}$, respectively. Additionally, we found that a 30 cm displacement for

the ^{125}I seed reduces the eye and skin doses by at least 3- and 2-fold, respectively. For future studies, a computational phantom can be utilized to monitor the dose to the eye and skin of personnel who are equipped with protective devices (such as lead glasses and an apron).

Conflict of Interest

No potential conflict of interest relevant to this article was reported.

Acknowledgements

I need to mention the efforts of our dear colleagues, Mr. Mohammad Reza Javanshir and Reza Naghdi who helped us, build the seed source.

Ethical Statement

This article does not contain any studies with human participants or animals performed by any of the authors.

Author Contribution

Conceptualization: Poorbaygi H, Salimi SM. Methodology: Poorbaygi H, Salimi SM. Formal analysis: Poorbaygi H, Torkzadeh F. Supervision: Poorbaygi H, Torkzadeh F, Hamidi S. Funding acquisition: Torkzadeh F, Sheibani S. Investigation: Poorbaygi H, Salimi SM, Torkzadeh F. Writing - original draft: Salimi SM. Writing - review & editing: Poorbaygi H. Approval of final manuscript: all authors.

References

1. Kim JH, Hilaris B. Iodine 125 source in interstitial tumor therapy. Clinical and biological considerations. *Am J Roentgenol Radium Ther Nucl Med.* 1975;123(1):163-169.
2. Shahzadi S, Azimi P, Parsa K. Long-term results of stereotactic brachytherapy (temporary 125iodine seeds) for the treatment of low-grade astrocytoma (grade II). *Iran Red Crescent Med J.* 2013; 15(1):49-57.
3. Ghassemi F, Sheibani S, Arjmand M, Poorbaygi H, Kouhestani E, Sabour S, et al. Comparison of iodide-125 and ruthenium-106 brachytherapy in the treatment of choroidal melanomas. *Clin Ophthalmol.* 2020;14:339-346.
4. Cattani F, Vavassori A, Polo A, Rondi E, Cambria R, Orecchia R, et al. Radiation exposure after permanent prostate brachythera-

- py. *Radiother Oncol.* 2006;79(1):65–69.
5. Anglesio S, Calamia E, Fiandra C, Giglioli FR, Ragona R, Ricardi U, et al. Prostate brachytherapy with iodine-125 seeds: radiation protection issues. *Tumori.* 2005;91(4):335–338.
 6. Kaulich TW, Lamprecht U, Paulsen F, Lorenz J, Maurer U, Loeser W, et al. Physikalisch-technische Qualitätssicherung und Strahlenschutz bei der Monotherapie der Prostata mit Jod-125-Seeds [Physical and technical quality assurance and radiation protection in transperineal interstitial permanent prostate brachytherapy with 125-iodine seeds]. *Strahlenther Onkol.* 2002;178(12):667–675 (German).
 7. Fujii K, Ko S, Nako Y, Tonari A, Nishizawa K, Akahane K, et al. Dose measurement for medical staff with glass dosimeters and thermoluminescence dosimeters during ¹²⁵I brachytherapy for prostate cancer. *Radiat Prot Dosimetry.* 2011;144(1–4):459–463.
 8. Schiefer H, von Toggenburg F, Seelentag W, Plasswilm L, Ries G, Lenggenhager C, et al. Exposure of treating physician to radiation during prostate brachytherapy using iodine-125 seeds: dose measurements on both hands with thermoluminescence dosimeters. *Strahlenther Onkol.* 2009;185(10):689–695.
 9. Al-Haj AN, Lobrigitto AM, Lagarde CS. Radiation dose profile in ¹²⁵I brachytherapy: an 8-year review. *Radiat Prot Dosimetry.* 2004;111(1):115–119.
 10. Classic KL, Furutani KM, Stafford SL, Pulido JS. Radiation dose to the surgeon during plaque brachytherapy. *Retina.* 2012;32(9):1900–1905.
 11. Souza DCB, Rostelato MEC, Vicente R, Zeituni CA, Tiezzi R, Costa OL, et al. Assessment of the risks associated with iodine-125 handling production sources for brachytherapy. 2015 International Nuclear Atlantic Conference (INAC); 2015 Oct 4–9; São Paulo, Brazil. Available from: https://inis.iaea.org/collection/NCLCollectionStore/_Public/47/035/47035623.pdf
 12. International Atomic Energy Agency. Implications for occupational radiation protection of the new dose limit for the lens of the eye: IAEA-TECDOC, no. 1731 [Internet]. IAEA; 2013 [cited 2023 Dec 12]. Available from: https://www-pub.iaea.org/MTCD/Publications/PDF/TE-1731_web.pdf
 13. Bahrudin NA, Hashim S, Karim MKA, Sabarudin A, Ang WC, Salehjon N, et al. Radiation dose to physicians' eye lens during interventional radiology. *J Phys Conf Ser.* 2016;694:012035.
 14. Netherlands Commission on Radiation Dosimetry. Guidelines for radiation protection and dosimetry of the eye lens [Internet]. Netherlands Commission on Radiation Dosimetry; 2018 [cited 2023 Dec 12]. Available from: <https://doi.org/10.25030/ncs-031>
 15. International Organization of Standardization. ISO 15382: Radiological protection: procedures for monitoring the dose to the lens of the eye, the skin and the extremities. ISO; 2015.
 16. International Radiation Protection Association. IRPA guidance on implementation of eye dose monitoring and eye protection of workers [Internet]. IRPA; 2017 [cited 2023 Dec 12]. Available from: [https://www.irpa.net/docs/IRPA%20Guidance%20on%20Implementation%20of%20Eye%20Dose%20Monitoring%20\(2017\).pdf](https://www.irpa.net/docs/IRPA%20Guidance%20on%20Implementation%20of%20Eye%20Dose%20Monitoring%20(2017).pdf)
 17. Wang B, Xu XG, Bozkurt A, Goorley JT. Issues related to the use of MCNP code for an extremely large voxel model VIP-Man. American Nuclear Society Topical Meeting in Monte Carlo; 2005 Apr 17–21; Chattanooga, TN, USA.
 18. Lohrabian V, Sheibani S, Aghamiri MR, Ghozati B, Poorbaygi H, Baghani HR. Determination of dosimetric characteristics of Ir-Seed ¹²⁵I brachytherapy source. *Iran J Med Phys.* 2013;10(2):109–117.
 19. Sheikholeslami S, Nedaie HA, Sadeghi M, Pourbeigy H, Shahzadi S, Zehtabian M, et al. Monte Carlo calculations and experimental measurements of the TG-43U1-recommended dosimetric parameters of ¹²⁵I (Model IR-Seed2) brachytherapy source. *J Appl Clin Med Phys.* 2016;17(4):430–441.
 20. Carrillo RE, Uribe RM, Woodruff GL, Stoebe TG. Lithium fluoride (TLD-700) response to a mixed thermal neutron and gamma field. *Radiat Prot Dosimetry.* 1987;19(1):55–57.
 21. Meigooni AS, Mishra V, Panth H, Williamson J. Instrumentation and dosimeter-size artifacts in quantitative thermoluminescence dosimetry of low-dose fields. *Med Phys.* 1995;22(5):555–561.
 22. Xu XG. An exponential growth of computational phantom research in radiation protection, imaging, and radiotherapy: a review of the fifty-year history. *Phys Med Biol.* 2014;59(18):R233–R302.
 23. James MR, McKinney GW, Durkee JW, Fensin ML, Hendricks JS, Pelowitz DB, et al. MCNPX 2.7.X: New features being developed LA-UR-09-6788. 2009 IEEE/NSS Conference; 2009 Oct 25–31; Orlando, FL, USA. p. 25–31.
 24. Martin CJ, Magee JS, Sandblom V, Almen A, Lundh C. Eye dosimetry and protective eyewear for interventional clinicians. *Radiat Prot Dosimetry.* 2015;165(1–4):284–288.